SINTEF

This is the accepted manuscript version of the article

The Synergistic Roles of Temperature and Pressure in Thermo-Compression Bonding of Au

Pranav Ambhore, Karthick Mani, Brett Beekley, Nishant Malikb Kari Schjølberg-Henriksen, Subramaniam Iyer and Mark S. Goorsky

Citation:
Pranav Ambhore, Karthick Mani, Brett Beekley, Nishant Malikb Kari Schjølberg-Henriksen, Subramaniam Iyer and Mark S. Goorsky, The Synergistic Roles of Temperature and Pressure in Thermo-Compression Bonding of Au. ECS Trans. 2018 volume 86, issue 5, 129-135, doi: 10.1149/08605.0129ecst .

This is accepted manuscript version.
It may contain differences from the journal's pdf version.

This file was downloaded from SINTEFs Open Archive, the institutional repository at SINTEF
http://brage.bibsys.no/sintef

The Synergistic Roles of Temperature and Pressure in Thermo-Compression Bonding of Au

P. Ambhore[1,2], K. Mani[1,2], B. Beekley[1], N. Malik[3], K. Schjølberg-Henriksen[4], S. Iyer[1,2], and M. S. Goorsky[1,2]

[1] Department of Materials Science and Engineering, University of California, Los Angeles, CA 90095, U.S.A.
[2] Center for Heterogeneous Integration and Performance Scaling (CHIPS UCLA), University of California, Los Angeles, CA 90095, U.S.A
[3] Centre for Materials Science and Nanotechnology, University of Oslo, 0316 Oslo, Norway
[4] SINTEF ICT, P. O. Box 314 Blindern, 0314 Oslo, Norway

Au-Au thermocompression bonding is a widely used technique for a variety of applications including hermetic sealing and packaging at a fine pitch. We have investigated the roles of pressure and temperature individually at different pressures (15 -100 MPa) and temperatures (150 and 250° C) of sputter deposited 1.2 µm thick Au thin films using a flattening technique. The initial surface root mean square (RMS) roughness of deposited films was 3-5 nm. Void morphology and the evolution of the interface was studied using atomic force microscopy. Power spectral density function plots were used to study variation in asperities at the surface. The void morphology and evolution was different when flattening and bonding at different temperatures and pressures.

Introduction

Thermocompression bonding is a bonding technique that has shown great potential to advance packaging in next-generation electronic circuits and devices. It overcomes most of the disadvantages of current industrial workhorses like conventional wire bonding, bumps, and Ball Grid Array (BGA) technologies. Fabricating pillars or structures and then bonding directly at the lowest possible temperature, time, and pressure at extremely fine pitches (<10 µm) is extremely desirable (1). These pillars can deliver power to any location on the circuit dies as opposed to wire bonding which can only access the pads along the die edges. Achieving fine pitch interconnects is very challenging in solder bonding technologies like BGA due to the initial large size of the solder bump (50-100 µm). Solder bonding technologies also have increased the potential of forming intermetallics at the interface thereby degrading the electrical and mechanical reliability of such joints (2)(3).

Thermocompression bonding can be used for any of the standard electrical conductors used in devices like Cu, Al, and Au. Au is an especially popular element for thermocompression bonding because it resists the formation of a native oxide on the surface. As the two bonding surfaces are pressed against one another, Au atoms from across the interface diffuse over and grains grow, provided temperature is sufficiently high. Pressure helps in bringing the two surfaces atomically closer and in plastically deforming the two surfaces locally. Temperature provides the requisite energy for atoms diffuse. It

also affects the mechanical properties of metals like yield strength and Young's modulus, both of which show an approximate 10% decrease as temperature increases from 150 to 250 °C for Au (5).

A low temperature, low pressure, short time and high output efficiency, high bond strength and 100% bonded interface area thermocompression bonding process is desirable. The aim of this study is to glean a better understanding of the impact of different factors (e.g. : pressure, temperature, roughness, time) on thermocompression bonding and this was pursued by using sputter deposited Au films. Our previous work (7) had shown that void morphology of bonded interface differed at different pressures and temperature even though the initial bonding surfaces were similar. This aim of this study is to isolate the roles of pressure and temperature by using Si dies which do not bond with Au surfaces. Bonded Au-Au structures were also studied using 1.2 µm thick films and characterized using X-ray diffraction, atomic force microscopy and focused ion beam (FIB) microscopy. In addition to this, unbonded Au films were studied individually with atomic force microscopy and X-ray diffraction and an attempt was made to individually assess the roles of pressure and temperature by studying roughness before and after flattening

Experimental

Two types of samples were prepared – 1.2 µm thick Au thin films, fabricated by SINTEF and their preparation and bonding procedure is described elsewhere (6). In brief, a 0.4 µm layer of what? was sputter deposited on a Si wafer followed by 1.2 µm of sputtered Au; some regions were patterned using lithography. The composition schematic for the samples is shown in Fig. 1. The Au frames used in the bonding study had inner dimensions of 3.34 x 3.34 mm^2 and the frame width was 40 µm. The bonding conditions and bonding at lower pressure is discussed elsewhere (7). The surface roughness was studied by taking 40x40 μm^2 scans of regions with blanket Au deposit using a Quesant Q-scope atomic force microscope. Further, the texture and grain sizes of the layers were determined using X-ray diffraction. X-ray diffraction data was collected using a Jordan Valley (now Bruker) diffractometer with incident parallel beam optics, Cu Kα radiation, and scattered beam slits. Bonded interfaces were studied using NOVA focused ion beam (FIB) scanning electron microscope (SEM). The parameters and procedure by which the interfaces were studied have been described in an earlier study (7).

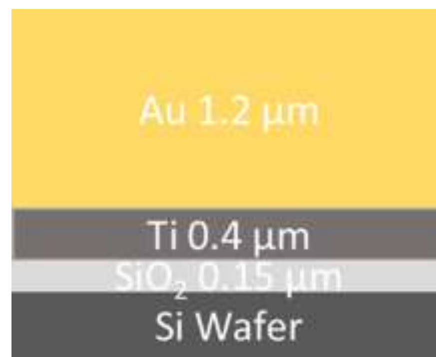

Figure 1. Cross-section showing layers and layer thicknesses in the sample

The role of pressure was studied using a flattening technique which involved pressing a square Si die (1x1, 2x2 mm^2) against the Au surface at different temperatures using a Kulicke & Soffa APAMA C2W bonder. The consequence of pressure is that surface roughness is reduced (9) which promotes bonding. A schematic of the flattening process is depicted in Fig. 2. Data for a flattening time of 180 seconds is provided at this juncture as it was observed that for longer flattening times (8 min), there were no further significant change in roughness. Flattening was performed at average interfacial temperatures of 150 and 250 °C and pressures were 15, 30, 60 and 100 MPa. These conditions were similar to bonding times used in our earlier work (7). The role of temperature was studied by annealing the samples at 150 and 250 °C for 10 and 30 minutes each. Surface diffusion constants at different temperatures and activation energy were extracted from line scans from AFM data and will be described in a future publication.

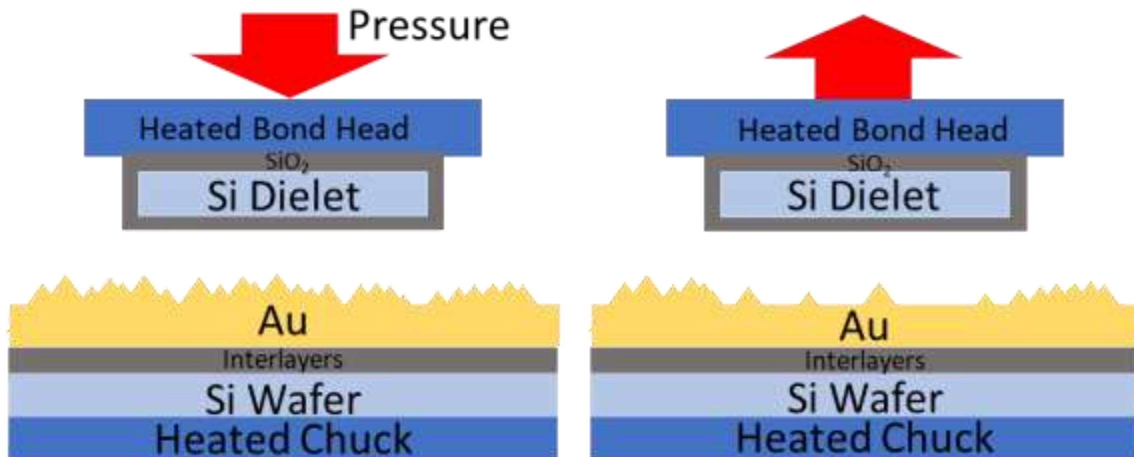

Figure 2. Flattening process

Statistical information from the AFM scans was gathered using Power Spectral Density Function (PSDF) plots. Gwyddion software (8) was used to extract these plots from AFM area scans. The x-axis in the PSDF plot represents spatial frequencies; high spatial frequencies represent small asperities while larger asperities correspond to smaller spatial frequencies. The y-axis in PSDF plots represents asperity content at a particular spatial frequency. If the surface roughness changes, particularly if it changes for some heights and not others, the content of spatial frequencies change, and this variation is represented conveniently in the PSDF plot.

Results and Discussion

Cross – section images of bonded interfaces of thicker 1.2μm films bonded at 150 °C and 250 °C and 14 MPa are shown in Fig. 3. It can be seen that as the bonding temperature increases, the fraction of voids at the interface decreases. The geometries of voids after bonding at 150 °C was found to be closely related to the initial surface roughness (7).

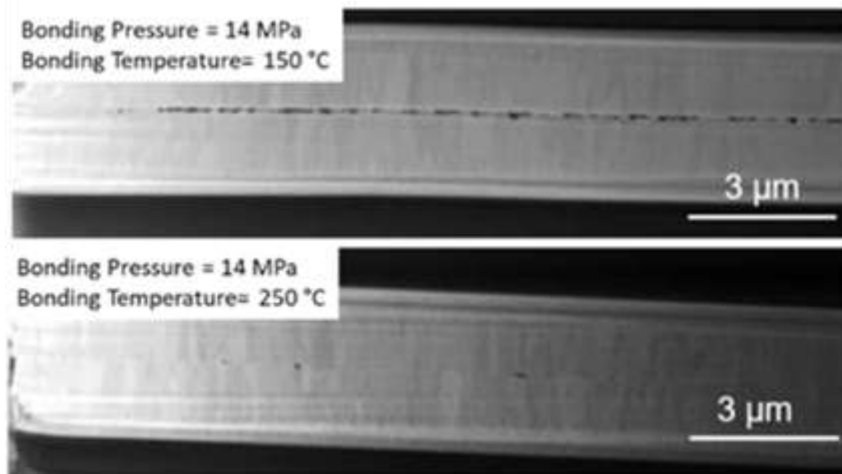

Figure 3. SEM cross-section of bonded interfaces at different temperatures.

It was observed that the void length decreased along the interface for both temperatures, however, the void height showed temperature dependence. The void height decreased when bonding at 250 °C. This decrease in void height was not observed for bonding at 3 MPa and therefore the reduction in void height can be attributed to pressure at 250 °C. These results can be understood through a combination of stress enhanced surface diffusivity due to higher pressure and decreased yield strength and elastic modulus with increasing bonding pressure and temperature (7)(10).

The initial RMS roughness of the Au films was 3-5 nm. The initial peak to valley heights of the unbonded thicker Au films were 20-30 nm and the correlation length was approximately 400 nm. These values match well with observed SEM images (7).

Flattening was studied over a wide range of pressures to include both the results from our previous study but also other studies that showed bonding at much higher pressures. The roughness values and percentage change in roughness can be observed in Fig. 4 and 5.

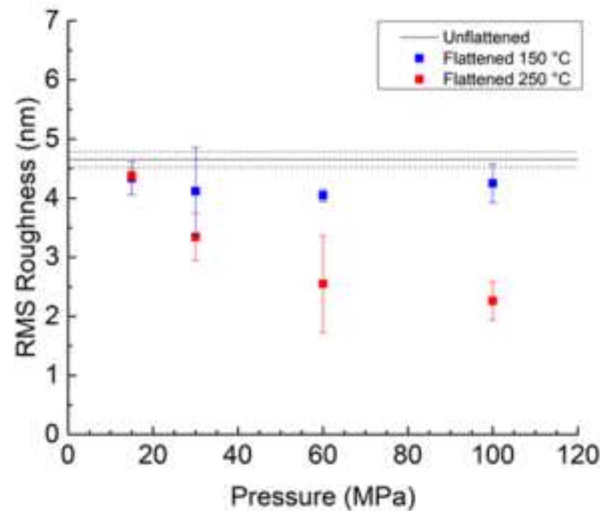

Figure 4. Roughness values before and after flattening at 150 and 250 °C (dotted lines are the standard deviation for unflattened sample)

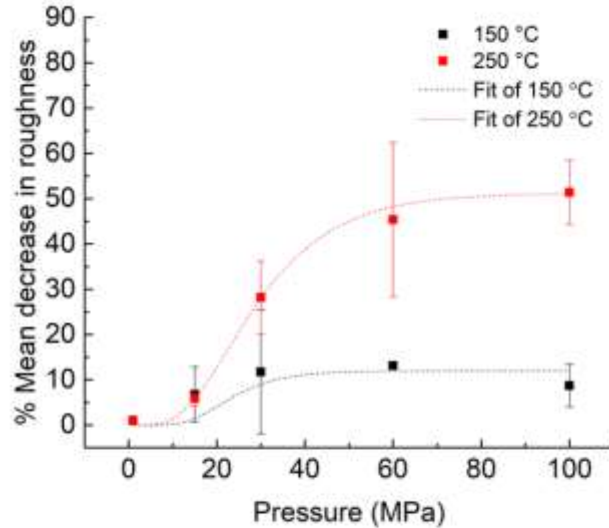

Figure 5. Percentage change in roughness after flattening at 150 and 250 °C.

The decrease in roughness when flattening at 250 °C can be understood in the following manner: The tallest peaks or features on the Au surface are contacted by the Si die first and start to deform plastically. These tall peaks are fewer in number, isolated and distributed across the surface. When the Si die presses against them, they start to reduce in height and therefore number. The apparent low pressure is sufficient to reduce their heights because stress is concentrated on a very small area, rather than the area of the die. Pressure up to this point is insufficient to deform the averagely sized peaks. The sudden decrease in roughness at intermediate pressures (15-60 MPa) is attributed to a small but uniform decrease in average-peak heights across the entire area of flattening. The initial low percent decrease in roughness at low pressure is because the number of tall peaks is low. When the averagely sized peaks start to reduce in height (> 15 MPa), even a small reduction in their heights across a 40x40 μm^2 area leads to significant reduction of roughness. At high pressure (100 MPa), it can be observed that reduction in roughness is nearly the same as that at 60 MPa. This can be attributed to the roughness of Si dies which was in the range of 1-2 nm and surface impurities. This behavior of drastic roughness reduction is not observed in samples flattened at 150 °C because the combination of pressure and temperature are insufficient to reduce the heights of averagely sized peaks in a significant manner.

PSDF for samples flattened at 150 and 250 °C, 100 MPa are shown in Fig 6. It can be observed that there is no reduction in asperities at 150 °C. However, at 250 °C, there is a reduction in the asperity content across the entire spectrum of spatial frequencies. As noted earlier, higher spatial frequency corresponds to smaller asperities.

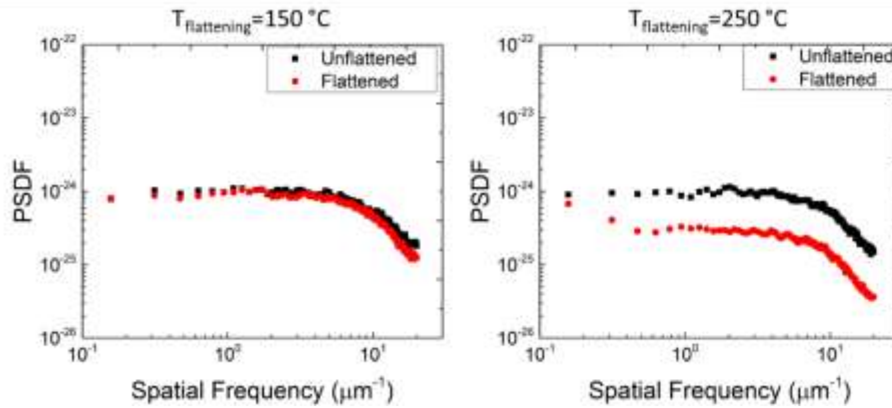

Figure 6. PSDF plots for $T_{flattening}$= 150 and 250 °C.

PSDF plots for annealing are shown in Fig. 7. It can be observed that 150 °C, there's no significant change in nature of plot at both the considered times i.e. 10 and 30 min. Similarly, when annealing was performed at 250 °C for 10 min, there was no measureable change in the PSDF plot. However, at 250 °C, when the annealing time is 30 min, a reduction in asperity content can be observed. The reduction in asperity content seems to be larger for high spatial frequency. Higher spatial frequency corresponds to smaller asperities. This can be understood based on the time and temperature dependence of diffusion. At lower temperature and shorter times, the Au atoms do not diffuse enough to significantly impact the PSDF. However, at higher temperatures – and and provided the Au atoms have sufficient time to diffuse – the asperity distribution at high spatial frequencies starts to alter. During annealing, the smaller asperities are reduced faster than larger asperities as fewer Au atoms are required to alter the morphology of smaller asperities. The content of larger asperities might also be affected for longer time scales than commonly used in thermocompression bonding and needs to be studied further.

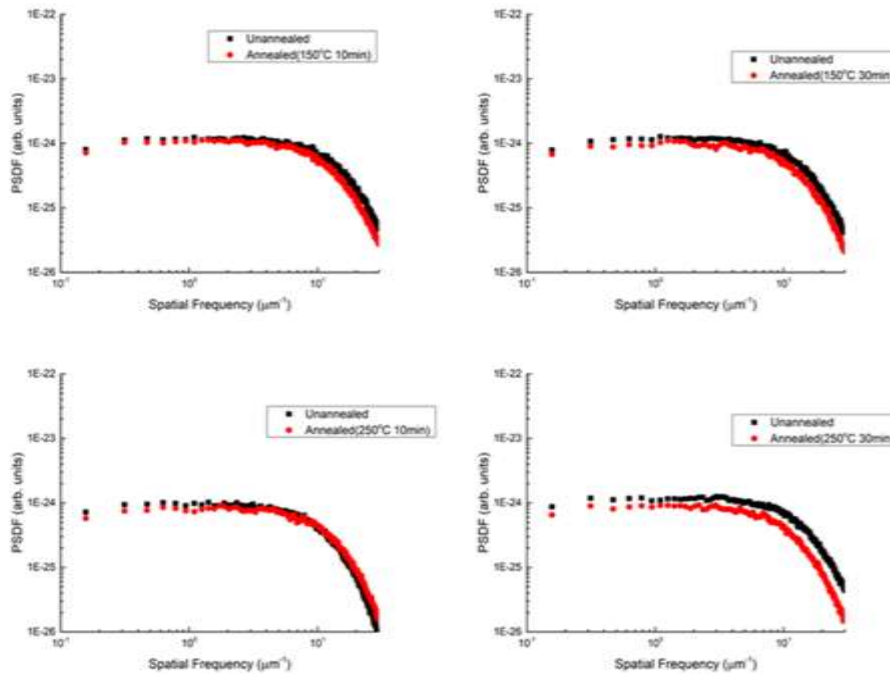

Figure 7: PSDF plots before and after annealing for 10 and 30

Conclusions

Au-Au thermocompression bonding was investigated for different bonding conditions (15-100 MPa; 150-250°C; 180 s). A combination of pressure and temperature is required to provide the requisite driving force for surfaces to deform plastically and come atomically closer for diffusion to occur across the bonding interface. It was found from PSDF analysis that temperature leads to a preferential reduction in high spatial frequency asperity content while flattening reduces asperities across the entire frequency spectrum.

Acknowledgments

SINTEF, Norway and UCLA CHIPS supported this work. The authors would also like to acknowledge the Research Council of Norway and ISNC-CNSI, UCLA.

References

1. A. A. Bajwa, S. Jangam, S. Pal, N. Marathe, T. Bai, T. Fukushima, M. Goorsky, and S. S. Iyer, IEEE 67th Electronic Components and Technology Conf., 2017, p. 1276
2. Y. Wang, D. T. Chu, and K. N. Tu, in IEEE 66th Electronic Components and Technology Conference, 2016, pp. 439–446.
3. N. Fu, J. C. Suhling, and P. Lall, IEEE 66th Electronic Components and Technology Conference. Las Vegas, NV, pp. 1119–1127, 2016.
4. L. Xie, S. Wickramanayaka, S. C. Chong, V. N. Sekhar, D. Ismeal, and Y. L. Ye, in IEEE 66th Electronic Components and Technology Conference, 2016, pp. 2126–2133
5. S. Collard, Ph.D. Thesis, Rice University (1991)
6. N. Malik, H. R. Tofteberg, E. Poppe, T. G. Finstad, and K. Schjølberg-Henriksen, ECS J. Solid State Sci. Technol. 4, P236 (2015)
7. M.S. Goorsky et al 2018 Jpn. J. Appl. Phys. 57
8. David Nečas and Petr Klapetek, Central European Journal of Physics 10 (2012) 181–188
9. Logeeswaran, V., Chan, ML., Bayam, Y. et al. Appl. Phys. A (2007) 87: 187
10. P. Gondcharton, B. Imbert, L. Benaissa, and M. Verdier, ECS J. Solid State 28 Sci. Technol. 4, P77 (2015)